



Universiteit  
Leiden  
The Netherlands

## **New neuroimaging approaches in Parkinson's disease**

Schipper, L.J. de

### **Citation**

Schipper, L. J. de. (2020, February 18). *New neuroimaging approaches in Parkinson's disease*. Retrieved from <https://hdl.handle.net/1887/85511>

Version: Publisher's Version

License: [Licence agreement concerning inclusion of doctoral thesis in the Institutional Repository of the University of Leiden](#)

Downloaded from: <https://hdl.handle.net/1887/85511>

**Note:** To cite this publication please use the final published version (if applicable).

Cover Page



Universiteit Leiden



The handle <http://hdl.handle.net/1887/85511> holds various files of this Leiden University dissertation.

**Author:** Schipper L.J. de

**Title:** New neuroimaging approaches in Parkinson's disease

**Issue Date:** 2020-02-18

# 6 Classification of Parkinson's disease status based on resting-state functional connectivity data

Sheila Rood<sup>1,2\*</sup>

Laura de Schipper<sup>3\*</sup>

Jeroen van der Grond<sup>4</sup>

Johan Marinus<sup>3</sup>

Johanna Henselmans<sup>3,5</sup>

Jacobus van Hilten<sup>3</sup>

Frank de Vos<sup>1,4,6</sup>

<sup>1</sup> Leiden University, Institute of Psychology, Department of Methodology and Statistics, Leiden, the Netherlands

<sup>2</sup> Leiden University, Faculty of Social and Behavioral Sciences, Leiden, the Netherlands

<sup>3</sup> Leiden University Medical Center, Department of Neurology, Leiden, the Netherlands

<sup>4</sup> Leiden University Medical Center, Department of Radiology, Leiden, the Netherlands

<sup>5</sup> Antonius Hospital, Department of Neurology, Woerden, the Netherlands

<sup>6</sup> Leiden University, Leiden Institute for Brain and Cognition, Leiden, the Netherlands

\* Joint first author



## ABSTRACT

**Introduction:** Recent research shows that resting-state fMRI data in combination with machine-learning techniques can be used to distinguish patients with neurodegenerative disease, like Alzheimer's disease, from healthy control subjects. We aimed to explore the potential of an elastic net model to recognize Parkinson's disease (PD) patients (at an individual level) using resting-state fMRI.

**Methods:** We used resting-state fMRI scans from 114 PD patients and 58 age- and sex-matched healthy control subjects. We calculated functional connectivity matrices and dynamics for full and partial correlations, resulting in four feature types, which have been used separately as well as combined in a cross-validated elastic net regularized logistic regression. We calculated the area under the curve to determine classification performance.

**Results:** The area under the curve values ranged between 0.752 and 0.858. Highest values were found for partial correlation functional connectivity dynamics. We also investigated whether particular clinical features contributed to the individual classification scores of PD patients and no associations were found.

**Conclusion:** These results show that resting-state functional connectivity dynamics in an elastic net regression is a promising method to differentiate between PD patients and healthy control subjects at an individual level.

## INTRODUCTION

Parkinson's disease (PD) is the most common neurodegenerative disorder after Alzheimer's disease (AD), and its prevalence is growing (De Rijk et al., 2000; Dorsey et al., 2018). The clinical spectrum of PD comprises a broad range of motor and non-motor symptoms (Chaudhuri et al., 2006). Patients show conspicuous differences in the course or occurrence of symptoms, the severity of symptoms, as well as in the progression rate of the disease (Foltynie et al., 2002). The heterogeneity of PD can complicate diagnosis in clinical practice. Adding to the complexity of early diagnosis is the long pre-symptomatic phase of the disease, when neurodegeneration has commenced, but the (motor) symptoms are yet insufficient to define PD (Berg et al., 2015).

Resting-state functional magnetic resonance imaging (fMRI) of the brain might have the potential to identify early PD or persons at risk, before overt expression of the disease. Resting-state fMRI data of PD patients have shown differences between PD patients and control subjects in functional connectivity (de Schipper et al., 2018). Furthermore, a recent study showed changes in PD patients in the variations of functional connectivity over a short time (dynamics) (Kim et al., 2017). However, these results represent group-wise comparisons and are not applicable to individual patients with PD. In AD, resting-state fMRI research has shown promising results in distinguishing patients and control subjects at an individual level through classification approaches that enable the incorporation of numerous functional connectivity parameters as predictors into one model and automatically select the most relevant ones (de Vos et al., 2018; Schouten et al., 2016).

The aim of the present study is to investigate whether resting-state fMRI data can be used to classify PD patients and healthy control subjects. We calculated whole-brain functional connectivity using full and partial correlations, and calculated functional connectivity dynamics using a sliding window approach (Hutchison et al., 2013). These features were used as input for machine-learning techniques to calculate classification scores for each measure (full and partial functional connectivity matrices and dynamics) separately and all measures combined in order to determine the most accurate prediction model. We further investigated whether classification scores were correlated to clinical measures of PD.

## **METHODS**

### **Study design and participants**

The sample for the current study consists of 172 participants: 114 PD patients, of which 11 patients were diagnosed as PD with Lewy bodies (DLB) subtype, and 58 healthy control subjects. In line with the most recent MDS-PD criteria, we qualified patients with DLB who met the clinical criteria for PD, as PD (Gibb and Lees, 1988; Postuma et al., 2015). Patients were recruited from the outpatient clinic for Movement Disorders of the Department of Neurology of the Leiden University Medical Center (LUMC; Leiden, the Netherlands) and nearby university and regional hospitals. PD patients fulfilled the United Kingdom Parkinson's Disease Society Brain Bank criteria for idiopathic Parkinson's disease (Gibb and Lees, 1988) and DLB patients the McKeith DLB diagnostic criteria for probable DLB (McKeith et al., 2005). Exclusion criteria were previous or other disorders of the central nervous system, peripheral nerve disorders influencing motor and/or autonomic functioning, and psychiatric comorbidity not related to PD. Control subjects were selected from the Leiden Longevity Study (Altmann-Schneider et al., 2013), matched at group level for age and gender with the PD patients.

### **Clinical measures**

The Movement Disorder Society unified Parkinson's disease rating scale (MDS-UPDRS) motor scale (part III) was used to quantify the severity of motor symptoms (Goetz et al., 2008). Fluctuating cognition and recurrent visual hallucinations are two core features of DLB, besides spontaneous features of parkinsonism (McKeith et al., 2005). We therefore included measures of cognition and hallucinations to our examinations as well. The mini-mental state examination (MMSE) was used to assess cognitive performance (Folstein et al., 1975). We quantified hallucinations using the hallucination item of the SCOPA psychiatric complications (PC, range: 0-18) scale (Visser et al., 2007). We further used the severity of non-dopaminergic symptoms in Parkinson's disease (SENS-PD) scale to measure symptoms that largely do not improve with dopaminergic medication (Goetz et al., 2008; van der Heeden et al., 2016). The SENS-PD is a composite score comprising three items with four response options (range: 0-3) from each of the following six domains: postural instability and gait difficulty, psychotic symptoms, excessive daytime sleepiness, autonomic dysfunction, cognitive impairment and depressive symptoms (total range: 0-54) (van der Heeden et al., 2016). These six domains represent a coherent complex of symptoms that may already be present in the early disease stages, and increases in severity when the disease advances (van der

Heeden et al., 2016). Higher scores reflect more severe impairment. The formula of Tomlinson et al. was used to calculate a levodopa equivalent dose (LDE) of daily levodopa (Tomlinson et al., 2010).

### **fMRI acquisition**

Imaging was performed on a 3 Tesla MRI scanner (Philips Achieva, Best, the Netherlands). Participants were instructed not to fall asleep during the scan and to lie with their eyes closed without moving. The following parameters were used for the resting-state fMRI scans: repetition time = 2.2 s, echo time = 30 ms, flip angle = 80°, 37 slices, resulting in a voxel size of 2.75 × 2.75 × 2.72 mm, with a 10% interslice gap, 200 volumes, scan duration 7 min and 29 s. Three-dimensional T1-weighted anatomical images were obtained with the following parameters: repetition time = 9.8 ms, echo time = 4.6 ms, flip angle = 8°, FOV 220 × 174 × 156 mm, 130 slices with a slice thickness of 1.2 mm with no gap between slices, resulting in a voxel size of 1.15 × 1.15 × 1.20 mm. A 32-channel and an 8-channel head coil was used for the PD group and the control group respectively.

### **Resting-state fMRI preprocessing**

Resting-state fMRI data was preprocessed applying: motion correction with the motion correction FMRIB's linear image registration tool (MCFLIRT) (Jenkinson et al., 2002a), brain extraction (Smith, 2002) and spatial smoothing using a Gaussian kernel with a full width at half maximum of 5 mm. Preprocessing further consisted of high-pass temporal filtering with a cutoff frequency 0.01 Hz and finally a non-linear registration with boundary-based registration to the 2 mm isotropic Montreal Neurological Institute standard space image (MNI; Montreal, QC, Canada) and a 10 mm warp resolution (Greve and Fischl, 2009), via the T1-weighted images, using high-resolution echo planar images for an additional registration step between functional images and T1-weighted images (Andersson et al., 2007; de Schipper et al., 2018). We further used independent component analysis based automatic removal of motion artifacts (ICA-AROMA) to identify and remove residual motion-related artifacts data (Pruim et al., 2015a, 2015b). The resting-state fMRI scan was subsequently weighted by a gray matter probability map, because neuronal activity predominantly takes place in gray matter voxels. The Harvard-Oxford cortical structural atlas (as provided by FSL version 5.0) was used to separate the preprocessed scans into 48 different brain regions. Time courses for each of the 48 brain regions were calculated for each subject, which were subsequently used in the functional connectivity analyses.

### Functional connectivity matrices

We used the time courses of the 48 brain regions to calculate functional connectivity matrices, using both full and sparse partial correlations. Whereas full correlations represent the total correlation between two brain regions, sparse partial correlations focus on the unique correlation between two regions (Peng et al., 2009). Sparse partial correlations were calculated using the graphical lasso algorithm implemented in R package "glasso" (Friedman et al., 2010). For each subject we calculated both full and sparse partial correlations between all pairs of brain regions, resulting in two functional connectivity matrices both consisting of  $(48 \cdot (48 - 1))/2 = 1128$  correlations.

### Functional connectivity dynamics

The dynamics of the above described functional connectivity matrices were calculated, using a sliding window approach (Chang and Glover, 2010; Hutchison et al., 2013; Jones et al., 2012), in which functional connectivity is calculated within a limited time window. This window was shifted over the total length of the scan and the standard deviation over all these windows was calculated. The size of the window was set at 11 scan volumes, which equals 24.7 seconds, and was slid one volume at a time. Functional connectivity dynamics was calculated for both the full and sparse partial correlation matrices, resulting in two functional connectivity dynamics matrices both consisting of  $(48 \cdot (48 - 1))/2 = 1128$  correlations.

### Statistical analyses

The full and partial functional connectivity and dynamical matrices were used as input for elastic net regularized logistic regression models in order to classify subjects as either control subject (0) or PD patient (1). Elastic net regularized logistic regression has been commonly used for neuroimaging classifications studies (de Vos et al., 2018; Schouten et al., 2016; Teipel et al., 2017, 2015). We performed elastic net regularized logistic regression with all feature types separately as input, as well as with all feature types combined. In elastic net regression, only the most relevant predictors will enter the regression model (Friedman et al., 2010; Zou and Hastie, 2005). Elastic net regression uses a combination of an L1-regularisation (lasso) (Tibshirani, 1996) and an L2-regularisation (ridge) (Hoerl and Kennard, 1970) and compromises between the two (Zou and Hastie, 2005). R package "glmnet" was used for the elastic net analyses (Friedman et al., 2010).

We used nested cross-validation to ensure that we were not overfitting the classification model. The inner cross validation loop was used to tune the sizes of the L1 and L2 penalties, and the ratio between those two penalties. The outer cross validation loop was used to train and evaluate the classification model. For both the inner and outer cross validation loop we used tenfold cross-validation, where the data was split repeatedly into ten percent test set and ninety percent training set, making sure each part of the data had been used as test set once. The training set in the outer cross validation loop was used for the inner cross validation loop (figure 1). The whole cross validation procedure was repeated ten times in order to reduce the variability resulting from the random partitioning of subjects into training and test folds.

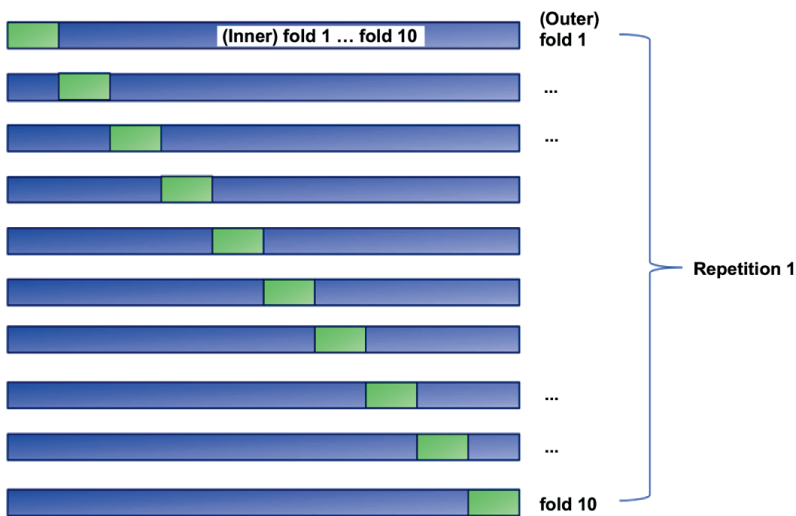


**Figure 1.** Cross-validation approach. Repeated, nested, tenfold cross-validation represented schematically. Green bars represent the test set, blue bars represent the training set. In reality, it was randomly chosen in which fold each of the subjects was part of the test or training set, making sure each of the subjects was only part of the test set once. For the purpose of the figure, however, the test and training set are portrayed as fixed blocks.

As the current study has an unbalanced design, we used receiver operator characteristic (ROC) curves to measure classification performance, as this method controls for unbalanced groups. The ROC curve was first computed and

subsequently the area under the curve (AUC) was calculated using the R-package "auc" (Balling & Van den Poel, 2013). Since there was no clear preference for a lower number of false positive diagnoses or a lower number of false negative diagnoses, the cut-off value to calculate the sensitivity and specificity was determined for each feature type individually, and was based on the Youden Index. This index reflects the value at which the sum of the sensitivity and the specificity is the highest (Fluss et al., 2005). The classification accuracy, sensitivity, and specificity were calculated for all features separately and combined.

Within the group of PD patients, we investigated the relationship between clinical variables (disease duration, MDS-UPDRS motor, SENS-PD and MMSE scores, hallucinations) and classification scores of the most accurate classification model using linear regression models (IBM SPSS Statistics for Mac, Version 23.0. Armonk, NY: IBM Corp.). The relationship between classification scores of the most accurate classification model and total LDE was investigated within the group of PD patients on dopaminergic medication. We also investigated group differences in classification scores of the most accurate classification model between drug-naïve patients and patients on dopaminergic medication using an independent-samples t-test. Bonferroni correction was applied in all cases.

## RESULTS

Demographic data of the PD patients and healthy control subjects and clinical data of the PD patients are shown in table 1. Gender and age did not significantly differ between the patient and control group.

### Classification accuracy

In table 2 the average AUC values over all cross-validation repetitions per feature type are shown. Combining all types resulted in an average classification accuracy of 0.818. Using the types of features separately resulted in a higher average classification accuracy for both partial correlation features, that is 0.832 for partial correlation functional connectivity and 0.858 for partial correlation functional connectivity dynamics, which is the highest AUC value obtained in the current study. Combining all types of features did not yield a higher AUC value than using all types of features separately. The individual predictions of the subjects are plotted in figure 2.

**Table 1.** Main characteristics of participants

	<b>Patients</b>	<b>Control subjects</b>
<b>N</b>	<b>114</b>	<b>58</b>
Men/women	74/40 (64.9)	31/27 (53.4)
Age, years	65.3 (7.0)	65.2 (7.5)
Disease duration, years	8.8 (4.7)	n/a
MDS-UPDRS motor score (0-132)	32.9 (15.3)	n/a
SENS-PD (0-54)	14.2 (6.4)	n/a
MMSE	28.0 (2.6)	n/a
SCOPA PC hallucination item (0-3)	4 <sup>a</sup>	n/a
Total LDE, mg/day <sup>b</sup>	954.9 (570.9)	n/a
Drug-naïve patients	20	n/a

Values are means (standard deviation) for continuous variables and numbers for gender (% men). For all measurement instruments, the score range is presented in parentheses. MDS-UPDRS: Movement Disorder Society unified Parkinson's disease rating scale; SENS-PD: severity of non-dopaminergic symptoms in Parkinson's disease; MMSE: mini-mental state examination; LDE: Levodopa dosage equivalent; n/a: not applicable.

<sup>a</sup> 4 Patients had a score > 1, range: 0–3; <sup>b</sup> N = 94 (20 patients were drug-naïve).

**Table 2.** Mean AUC, sensitivity and specificity

	<b>FFC</b>	<b>PFC</b>	<b>FFD</b>	<b>PFD</b>	<b>All</b>
AUC	0.752	0.832	0.753	0.858	0.818
Sensitivity	0.655	0.828	0.709	0.809	0.831
Specificity	0.781	0.778	0.744	0.822	0.705

AUC: area under the curve; FFC: full correlation functional connectivity; PFC: partial correlation functional connectivity; FFD: full correlation functional connectivity dynamics; PFD: partial correlation functional connectivity dynamics; All: FFC, PFC, FFD and PFD combined.

### Correlations with clinical scores

We investigated the relationship between individual elastic net partial correlation functional connectivity dynamics classification scores of the PD patients and clinical variables, but after correction for multiple comparisons, no statistically significant associations were found. The mean classification scores between drug-naïve patients (0.77) and patients on dopaminergic medication (0.83) did not significantly differ between groups ( $p = 0.205$ ).

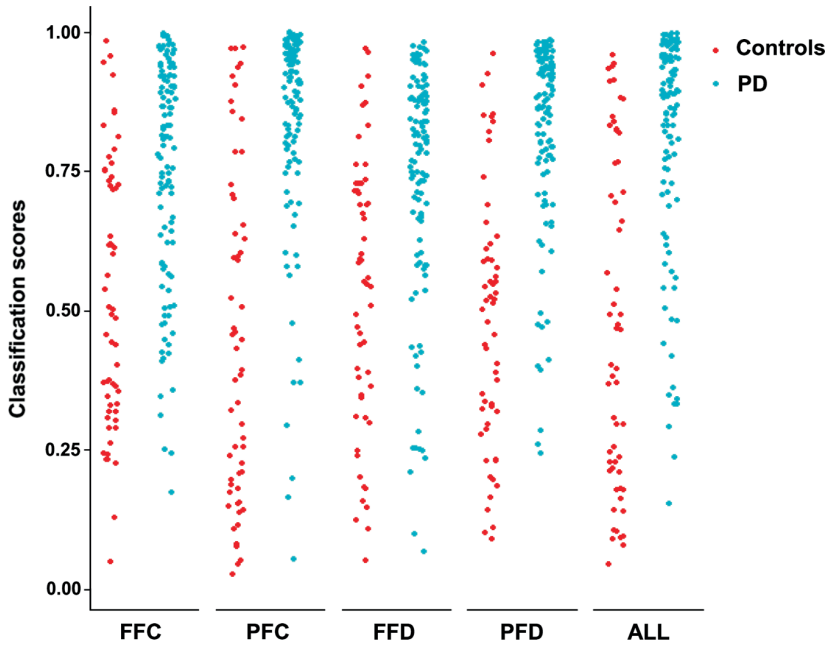


**Figure 2.** Classifications per feature type against diagnosis. FFC = full correlation functional connectivity, PFC = partial correlation functional connectivity, FFD = full correlation functional connectivity dynamics, PFD = partial correlation functional connectivity dynamics, ALL = FFC, PFC, FFD and PFD combined.

## DISCUSSION

We studied the accuracy of different resting-state fMRI measures in combination with machine-learning techniques for the (individual) classification of PD patients. Full and partial functional connectivity matrices and dynamics were computed and used as input in an elastic net regression to discriminate PD patients from healthy control subjects. For both the functional connectivity matrices and dynamics, partial correlations resulted in higher classification accuracy than full correlations. The functional connectivity dynamics resulted in a (slightly) higher classification accuracy than the functional connectivity matrices. Combining multiple feature types did not improve the classification accuracy compared to using the features separately.

The partial functional connectivity dynamics model resulted in an AUC of 0.86. Previous MRI studies that investigated machine learning techniques in PD,

have used T1-weighted MRI data for differentiation of PD from control subjects, patients with progressive supranuclear palsy or subjects with scans without evidence of dopaminergic deficit (SWEDD) (Sakai and Yamada, 2018). Previous studies using grey and white matter volumes of regions of interest for differentiation of PD and control subjects reported an overall accuracy 0.82 (Adeli et al., 2016) and 0.71 (Liu et al., 2016). Another study used T1-weighted MRI data alone as well, but incorporated structural connectivity between brain regions, and found an overall accuracy of 0.86 (Peng et al., 2017). A proposed approach for early diagnosis of PD that combined T1-weighted MRI markers with clinical scores typical of prodromal PD even reached an AUC value of 0.97 (Amoroso et al., 2018). Overall, the findings of these studies combined with our results, suggest that a combination of structural and functional imaging combined with machine learning approaches are a promising classification method for PD diagnosis, and in time possibly early or prodromal PD. The integration of other imaging modalities, such as diffusion tensor imaging (DTI), may further improve classification performances.

The dynamic changes of functional connectivity, which is relatively new in the field of PD, resulted in the highest classification accuracy. In a recent study, functional connectivity dynamics suggested two distinct connectivity states: a more frequent, sparsely connected within-network state and a less frequent, more strongly interconnected between-network state (Kim et al., 2017). Their results show that PD patients spent less time in the sparsely connected state, while they spent more time in the more strongly interconnected state (Kim et al., 2017). This suggests that the connectivity state that is characterized by increased interactions between cerebral networks predominates in PD, at the expense of the more sparsely within-network state (Kim et al., 2017). Our findings stressing the relevance of dynamic changes in classifying patients with PD are in line with those from previous studies in AD (de Vos et al., 2018; Jones et al., 2012). Functional dynamics may reflect aspects of functional capacity of neural systems (Deco et al., 2011; Kucyi et al., 2017), and are suggested as possible biomarkers of disease (Kim et al., 2017).

For both the functional connectivity matrices and dynamics, partial correlations resulted in higher classification accuracy than full correlations. As partial correlations are controlled for the potential effect of other brain regions on that relation (Peng et al., 2009), they provide unique information of the relationship between two brain regions and functional connectivity measures based on partial correlations therefore likely provide a better estimation of functional connectivity than full correlations (Smith et al., 2011).

Although the AUC value obtained for the functional connectivity dynamics model based on partial correlations in the current study was quite high, no associations with clinical variables were found. This may be attributed to the fact that the model was trained to differentiate PD patients from healthy control subjects, using a combined set of predictors selected from correlations between multiple brain regions, and classification scores. In turn, this approach renders the occurrence of correlations between partial functional connectivity dynamics and individual symptoms or clinical domains less likely.

This is the first study using resting-state fMRI data in combination with elastic net regression analysis for (individual) classification of PD patients, resulting in moderate to good PD classification. Machine-learning methods could be of use for early diagnosis of PD, or possibly detect brain changes in persons at risk for developing PD. However, the patient group used to train and test the prediction models in this study included few de novo PD patients, had a moderate mean disease severity and a mean disease duration of approximately nine years. A population comprising a larger number of de novo patients is possibly more suitable for the purpose of early diagnosis of PD. Further, 92 patients in this study were scanned while taking their usual dopaminergic medications, while 20 patients were drug-naïve. The acute effect of dopaminergic medication may normalize functional connectivity in PD (Tahmasian et al., 2015), and its chronic use may alter brain organization (Anderson and Nutt, 2011; Kaasinen et al., 2003). Dopaminergic medication was not related to the classification scores of our partial functional connectivity dynamics model, and mean classification scores did not differ between patients on dopaminergic medication and those who were not, but we cannot rule out a potential modulatory role of dopaminergic medication. A potential limitation of our study could be that the MRI acquisition of our two cohorts (control persons and patients with PD) were performed with a different type of head coil (8-channel versus 32-channel, respectively) (Panman et al., 2019), which might have affected our classification score, although another study comparing resting-state fMRI data using an 8- and 32-channel head coil on a 3 Tesla MRI scanner did not find significant differences between the two head coils (Paolini et al., 2015). Of note is that the scans in this study last 7 minutes and 29 seconds, and a timeframe of 24.7 seconds was taken as one window in the sliding-window approach, which is quite short to calculate functional connectivity dynamics (Hindriks et al., 2016). There exists an arbitrary trade-off between the number of measurement moments in one window and the number of different windows that can be used for calculation of functional connectivity dynamics. In the current study, using a higher number of

different windows was preferred over using more measurements in one window. However, using larger windows may yield even better classification accuracies than the ones that we found in the current study (Shirer et al., 2012).

### **Conclusion**

We showed that it is possible to achieve moderate to good PD classification using elastic net regularized logistic regression combined with resting-state fMRI data, in particular with partial functional connectivity dynamics. This approach has potential as a suitable method for use in future PD classification studies.